Implications of Global Atmospheric Spatial Spectra for Processing and Displaying Data

KEVIN E. TRENBERTH AND AMY SOLOMON*

*National Center for Atmospheric Research,** Boulder, Colorado*

(Manuscript received 24 January 1992, in final form 15 June 1992)

ABSTRACT

The information available on different scales in the atmosphere for a number of different variables is explored using the global ECMWF analyses by examining the spatial spectra at T106 resolution. In most atmospheric spectra, a low wavenumber regime can be identified that does not follow a power law and is dominated by the stationary forced part of the flow. A higher wavenumber regime, where an approximate power law does appear to hold, can also usually be found. For the rotational part of the flow in the upper troposphere, the observed spectra follow quite closely that expected for quasi-two-dimensional geostrophic turbulence between about wavenumbers 12 and 70, with a kinetic energy spectrum falling off as n^{-3}, where n is the total spherical harmonic wavenumber. In the lower troposphere, there is more power at high wavenumbers than would be expected from geostrophic turbulence, most likely due to the influence and close proximity of the lower boundary. Changes in the global analyses since 1979 have mainly influenced the spectra in the lower troposphere and the more recent analyses for 1988 have more power at higher wavenumbers. In the stratosphere, the spectra at high wavenumbers do not follow a power law behavior very well.

The widespread practice of using a coarse grid without the appropriate truncation or smoothing first can result in unresolved scales being aliased and excessively noisy fields; an example is the 2.5° gridded fields made available by ECMWF. Appropriate procedures are described for truncating the T106 ECMWF spectral archive for scalar and vector fields. T42 resolution is an adequate representation for diagnostic calculations depicting most quantities within a few percent accuracy, although some spatial structure, which may partly be noise, is lost for the ω, divergence, and moisture fields. In contrast, errors greater than 10% can occur at T21 or R15 resolution, although these truncations can be useful for displaying results.

1. Introduction

Questions often arise concerning what resolution is needed to compute various climate diagnostic quantities and how the results should be displayed. The answers depend very much on the quantities involved. It is quite common practice to smooth the results of calculations so that the large-scale features of interest are revealed and, indeed, the quality of figures published in journals is often greatly enhanced by applying a smoother of some kind to a field before it is plotted for presentation. Nearly always, however, the decision on whether and how much to smooth is purely ad hoc and depends on the subjective evaluation of the investigator. The goal, presumably, is to smooth sufficiently to suppress the noise in the field while retaining as much as possible the signal. Noise in this sense is often synonymous with unwanted small-scale structure, which, nevertheless, may be real and in some other contexts may be a signal of interest in its own right. On the other hand, it may indeed be a form of real noise, such as arises computationally from finite-difference techniques applied on a finite grid in which spurious two-delta wavelength features are apt to show up following certain calculations.

Dealing with noise and small-scale structure properly can be difficult; problems arise when the small scales are aliased onto the larger scales. This is apt to happen when information is available only on a very fine high-resolution grid but the user wishes to use (or has the capability of using) only a much coarser grid for diagnostic calculations. Under these circumstances it is important for the user to know something about the underlying structure in the data. Several questions arise as to whether it is best to interpolate as accurately as possible to the new grid; or should an area-averaged value be taken at each new grid point; or should some other form of smoothing be applied first? The answers depend on the variable in question; the important statistical property is the spatial wavenumber spectrum, as will be shown here. In particular, knowledge of the spatial scales present in the data and whether those can be resolved by the new grid is critical. If there is significant variance contained in unresolved scales,

* Present affiliation: Center for Meteorology and Physical Oceanography, Massachusetts Institute of Technology, Cambridge, Massachusetts.

** The National Center for Atmospheric Research is sponsored by the National Science Foundation.

Corresponding author address: Dr. Kevin E. Trenberth, National Center for Atmospheric Research, P.O. Box 3000, Boulder, CO 80307.

© 1993 American Meteorological Society

smoothing or weighted averaging of the original data in some form is essential if aliasing is not to become a problem. The following is an illustration of this point.

At the European Centre for Medium-Range Weather Forecasts (ECMWF) global analyses of atmospheric variables have been performed at T106 resolution. In this notation the "T" refers to triangular truncation at 106 wavenumbers using a spherical harmonic representation. For example, a variable ψ (the streamfunction) is represented as a finite sum:

$$\psi(\lambda, \phi, t) = a^2 \sum_{m=-J}^{J} \sum_{n=|m|}^{J} \psi_n^m(t) Y_n^m(\lambda, \phi), \quad (1)$$

where λ is longitude, ϕ is latitude, t is time, a is the radius of the earth, and

$$Y_n^m(\lambda, \phi) = P_n^m(\phi) e^{im\lambda} \quad (2)$$

are spherical harmonics of order m and degree n, and J is the truncation wavenumber. In (1) m is the east–west wavenumber and $l = n - |m|$ is the number of zeros between the poles and thus relates to the north–south wavenumber. The P_n^m are associated Legendre functions of order m and degree n. Triangular truncation is isotropic in the sense that every position and direction on the sphere is treated identically and, as n is a measure of both the zonal and meridional wavenumber, it is often referred to as the total wavenumber. Note that the Laplacian takes an especially simple form in spherical harmonics so that the vorticity is

$$\zeta = \nabla^2 \psi = - \sum_{m=-J}^{J} \sum_{n=|m|}^{J} n(n+1) \psi_n^m(t) Y_n^m(\lambda, \phi), \quad (3)$$

and thus the coefficient for vorticity:

$$\zeta_n^m = - \frac{n(n+1)}{a^2} \psi_n^m.$$

In this case, the representation of ψ is in spectral space, but to take advantage of Gaussian quadrature it is also common to depict the field on a Gaussian grid in which there are $M \geq 3J + 1$ equally spaced longitudes and $N \geq (3J + 1)/2$ Gaussian latitudes. As long as these inequalities hold it can be shown for the representation of quadratic products that the first J harmonics do not contain aliased information while the remaining discarded harmonics do. Washington and Parkinson (1986) discuss most of these aspects in considerable detail, including the choice of the Gaussian latitudes. One advantage of the Gaussian grid representation is the ability to use so-called spectral-transform techniques in which, given a truncation, the process of going back and forth is fully reversible.

For T106 representation the Gaussian grid required is 320 by 160 points and corresponds approximately to a 1.125° grid. Incidentally, the truncation wavenumber is chosen together with the selection of the grid size, which is usually selected to have dimensions that are factors of 2, 3, and 5 so that fast Fourier transform techniques can be applied when going back and forth from spectral to gridpoint space.

For climate purposes, because there are 14 levels of data and a number of variables at each level, there is a major burden in having to deal with the full T106 resolution. Accordingly, we wish to know, how much information is really contained in the high wavenumbers? Experience indicates that for geopotential height there is not much information expected beyond perhaps wavenumber 30 or so. After all, the synoptic network has upper-air observing stations spaced every few hundred kilometers or so at best over land, and much farther apart over the oceans, so that wavelengths less than about 1000 km cannot be resolved. This corresponds to zonal wave 40 at the equator or about wave 28 in midlatitudes. At the National Center for Atmospheric Research we have therefore made most use of the data at T42 truncation, corresponding to a grid of size 128 by 64 and about a 2.8° resolution. Methods for truncating the ECMWF spectral data are given in section 3.

The global ECMWF analyses at T106 resolution are being made available as a "WCRP[1]" dataset with the variables in spectral coefficient form. A package of software is made available by ECMWF to unpack the data and set up values on a regular grid of any chosen size. It is straightforward to modify this to also put out the variables on any Gaussian grid. Using this software the value assigned to each grid point is the exact value at T106 resolution or, in other words, a perfect interpolation has been made to the specified grid. But if a coarse grid, such as a 2.5° grid, is chosen the resulting field will be aliased when used for further processing on this grid.

The WCRP dataset is also made available on a 2.5° grid by ECMWF. Tests conducted have confirmed that these gridpoint values were produced using the above method, so that the gridpoint values are determined from the full T106 resolution. But because about twice as many grid points are needed to adequately depict the scales in each field at this resolution, the values are not representative of the 2.5° grid size.

One purpose of this paper is to check on the adequacy of this and other resolutions for representing various fields, to document the effects of aliasing when a coarse grid is used without the appropriate truncation or smoothing first, and to describe methods of truncating and smoothing fields for making computations and presenting results. A second purpose is to update the spectral description of the data from global analyses in the context of the appropriate theory by using more

[1] The dataset is made available through the World Climate Research Programme as part of the Tropical Oceans Global Atmosphere (TOGA) Programme.

recent data at much higher resolution, and to include many more variables than have been analyzed in the past.

2. Spatial spectra of atmospheric variables

We first address the question of how much information there is on different scales for a number of different variables in the global ECMWF analyses. To do this, the spatial spectra at T106 resolution are examined. The spectra reveal how much power, or variance per unit wavenumber, there is and so depict the relative importance of the different scales.

A relevant question is whether these spectra truly represent the real world, and the answer is that they almost certainly do not, at least in detail. The reason is that, as noted above, the information available from the observational network peters out on scales smaller than a few hundred kilometers, so that the analyzed small scales arise from the four-dimensional assimilation process. The latter is a system in which multivariate observed data are combined with the "first guess" using an approximation to a statistically optimum scheme. The first guess is the forecast of the current state of the atmosphere from previous analyses produced using a numerical weather prediction (NWP) model. Consequently, the primary source of the small-scale information is coming from the NWP model. It is therefore very much dependent on the formulation of things such as horizontal and vertical diffusion in the model and how the earth's surface is depicted. Nevertheless, it is the best available representation of what the real atmosphere is, and it is believed to be very realistic in many respects. Boer and Shepherd (1983) have previously examined spectra of global variables as seen in several analyses using data from the First GARP Global Experiment but included wavenumbers only out to $n = 32$. As will be shown, improvements in the analyses that have taken place since 1979 have changed the spectra somewhat to be more in line with theoretical considerations.

a. Theoretical spectra

There is a considerable amount of theory of two- and three-dimensional turbulence and the nature of the spectrum of kinetic energy that follows from the various assumptions in that theory. Tennekes (1978) introduces and discusses these aspects at a fairly elementary level. Boer and Shepherd (1983) summarize the implications for large-scale two-dimensional turbulence very nicely and go into considerable detail on the implications for the spectra.

Fundamentally, the arguments revolve around the relevance of two- versus three-dimensional turbulence and whether there is an energy and/or enstrophy cascade. For atmospheric waves, it is expected that there is a source wavenumber region which occurs at the larger scales. The sources include large-scale heating, land–sea contrasts, and orography that give rise to the quasi-stationary waves, and the baroclinically unstable waves. The sink for atmospheric energy in the free atmosphere is expected to be at the very high wavenumbers where ultimately molecular viscosity comes into play. Consequently, in three-dimensional turbulence, there is expected to be an "energy cascade" from low to high wavenumbers of energy. The wavenumber region between the sources and sinks is then dominated by inertial effects in which the nonlinear interactions associated with advection come into play. Kolmogorov's (1941) equilibrium theory can then be used for the inertial subrange to deduce that for three-dimensional turbulence the kinetic energy spectrum should be dominated by a $-5/3$ power law in which the kinetic energy falls off with higher wavenumber k such that the kinetic energy per unit wavenumber k is proportional to $k^{-5/3}$.

In contrast to three-dimensional turbulence, Charney (1971) has argued that the atmosphere is quasi–two dimensional because of its quasigeostrophic nature. As a result there is no energy cascade. For barotropic flow, there is conservation of enstrophy in two-dimensional inviscid flow and the dynamics are then controlled by vorticity conservation. Thus, enstrophy, which is one-half the square of the vorticity, should cascade from larger to smaller scales because of nonlinear random advection through an inertial subrange between the enstrophy source at low wavenumbers and the enstrophy sink at high wavenumbers, where enstrophy should be destroyed by microscale turbulence and molecular diffusion. In this case the kinetic energy per unit wavenumber is proportional to a k^{-3} and the spectrum has a -3 slope. Also, we can replace k with n. Charney (1971) noted that the kinetic energy and available potential energy equations combine in quasi-geostrophic flow to give a total energy equation that is analogous to the kinetic energy equation in two dimensions. Accordingly, it follows that both kinetic energy and available potential energy should exhibit a -3 spectrum in the inertial subrange.

While these are idealizations, they provide some guidance as to what the shape of the spatial wavenumber spectrum might look like in the free atmosphere. Near the surface, on the other hand, it might be expected that the spectrum more closely depends on the surface conditions because there are sources and sinks at all scales. Tennekes (1978) argues that the $-5/3$ law is more appropriate in the boundary layer and on small scales such as in convective clouds. Shepherd (1987) has examined the energy and enstrophy cascades from January 1979 global analyses and notes that the shapes of the kinetic energy spectra are consistent with expectations from the simple two-dimensional homogeneous turbulence theory whereas many assumptions of that theory are violated in practice. In particular, he points out that the theory should apply

to transient waves whereas interactions between transient and stationary waves are prominent in the observed spectral transfers. He nevertheless finds that the processes involved in the nonlinear interactions are mostly those included in the two-dimensional theory. Gage and Nastrom (1986) examined wind and temperature spectra from commercial aircraft measurements in the upper troposphere and lower stratosphere and found a -3 spectrum at wavelengths from several hundred to several thousand kilometers, but with the spectrum featuring a shallower slope of $-5/3$ for wavelengths shorter than 100 to 500 km.

In most atmospheric spectra, a low wavenumber regime can be identified that does not follow a power law in which the spectra fall off with n as n^{-b}, where b is the slope on a log–log plot, and is often dominated by the stationary forced part of the flow. We can often also identify a higher wavenumber regime where an approximate power law does appear to hold and, in some cases, it may be appropriate to interpret this as the inertial subrange.

As a guide, therefore, assuming the -3 power law for kinetic energy (or strictly speaking, the rotational kinetic energy) is appropriate, the power law expected for several other parameters can be estimated as follows.

The velocity $\mathbf{v} = (u, v)$ can be broken up into rotational and divergent parts involving the streamfunction, ψ, and the velocity potential, χ: $\mathbf{v} = \mathbf{k} \times \nabla\psi + \nabla\chi$, and the divergence is given by $\delta = \nabla^2\chi$. Accordingly, the kinetic energy (KE) may be broken up into rotational and divergent parts: $\mathrm{KE} = \mathrm{KE}_r + \mathrm{KE}_D$.

From (1) it can be shown (e.g., Boer and Shepherd 1983) that

$$\overline{\mathrm{KE}_r} = \frac{1}{2} a^2 \sum_{m=-J}^{J} \sum_{n=|m|}^{J} n(n+1)\psi_n^m \bar{\psi}_n^{-m}, \quad (4)$$

where the overbar indicates the global average and use has been made of the orthogonality of the spherical harmonics in performing the global integral. Similar expressions to (1), (3), and (4) apply for the divergent part of the wind except with χ, δ, and $\overline{\mathrm{KE}}_D$ replacing ψ, ζ, and $\overline{\mathrm{KE}}_r$.

For n large, $n(n+1)$ is similar to n^2 and the slope as a function of n is the same. Thus given a -3 slope for the spectrum for KE_r, from (4) the streamfunction should follow a -5 power law. From (3) the power law for vorticity, or effectively the enstrophy, should have a -1 slope.

From the geostrophic relation, the geopotential height might then be expected to also follow a -5 power law. However, to formalize this relation on a sphere, we make use of the linear balance equation

$$\nabla^2\Phi = \nabla \cdot f\nabla\psi. \quad (5)$$

If the geopotential height z is expressed in a spherical harmonic expansion as in (1) except without the a^2 factor, then (5) can be expressed in spherical harmonic coefficients [using (1)] as

$$z_n^m = \frac{(n+1)}{n} c_n^m \psi_{n-1}^m + \frac{(n+2)}{(n+1)} c_{n+1}^m \psi_{n+1}^m, \quad (6)$$

where we have defined

$$c_n^m = \frac{2\Omega a^2}{g} \cdot \left[\frac{(n-m)(n+m)}{(2n-1)(2n+1)}\right]^{1/2}.$$

The derivation of (6) takes advantage of several recurrence relations among Legendre functions, along with their orthogonality (see appendix of Trenberth 1973). For large n, $c_n^m \to \Omega a^2/g$, so that for large n (in practice values larger than about 10), the power in z_n^m is expected to follow that in ψ_n^m and thus follow a -5 power law.

As the spatial variance of temperature is the dominant factor in the expression for the available potential energy, it follows that temperature should also follow a -3 power law. For the divergent part of the flow, it is much less clear what model might be appropriate. For three-dimensional isotropic turbulence the divergent kinetic energy would follow a $-5/3$ law, in which case the divergence would follow a $+1/3$ power law and the power would actually be expected to increase slightly with wavenumber. In this case, because the vertical motions are comparable to the horizontal motions, ω would also follow a $-5/3$ law.

b. *ECMWF spectra*

We now present spectra of the relevant global variables from the ECMWF analyses for January and July of 1988. For an evaluation of the quality of the ECMWF analyses, see Trenberth and Olson (1988a,b) and Trenberth (1992). The latter discusses the changes in ECMWF analyses since 1979, which was the period used by Boer and Shepherd (1983).

We present spectra showing the power, that is, the variance per unit wavenumber, for the total wavenumbers 1 to 100. Spectra were computed for all 106 wavenumbers available but there was evidence of some problems at very high wavenumbers near the truncation limit, where an abrupt increase in power is found for some spectra. This behavior may be due to aliasing in which higher wavenumbers not resolved are projected onto these modes,[2] but it may also arise from the NWP model itself from "spectral blocking," in which the absence of processes associated with the higher wavenumbers and inadequate compensating dissipation leads to a buildup in power near the truncation limit (e.g., Boville 1991). Examples of this can

[2] See Gray and Madden (1986) for a discussion of the effects of aliasing on spectra and the folding of unresolved frequencies to lower frequencies thereby producing an aliased spectrum.

be seen, for instance, in the geopotential height spectra at 200 and 10 mb, presented later in Fig. 2.

Spectra have been computed for each time 0000 and 1200 UTC and each day for the months of January and July 1988 plus several other months and averaged to give the time-averaged spectrum (labeled "total"). Also computed were the spectra of the monthly mean time-averaged flow (labeled "mean") which therefore reveals the power in the stationary part of the flow, while the difference from the total gives the transient variance. The stability of each spectral estimate clearly depends on wavenumber. At high wavenumbers, where the transients dominate and the time scales are short, there are over 60 sample values. However, stationary or quasi-stationary components tend to dominate the very low wavenumbers so the daily spectral estimates are not independent. To gain some idea of how stationary the spectra are and indicate whether the one-month stationary component is simply a very low-frequency fluctuation, some results are presented for other years. To further help interpret the results, the two-dimensional spectra as a function of both m and n have also been computed, but these are not shown.

Figure 1 presents the spatial spectra of the geopotential of the fixed surface topography. Note that the plot has a log–log scale. The surface topography is not obviously directly relevant for interpreting the results in the atmosphere because geopotential heights in the free atmosphere do not follow that of the surface. As in mean sea level pressure calculations, the regions below ground are effectively replaced by an equivalent atmospheric mass as far as the free atmosphere is concerned. However, high orography does impact the atmosphere by forcing stationary planetary waves, and the transient flow is influenced by weather systems interacting with the complex surface topography. Note that the maximum power in Fig. 1 is at waves 3, 4, 5, and 6. Although there is a notable falloff in power with wavenumber, it does not follow a power law and the rate of falloff is closer to n^{-2}, which is much less than the n^{-5} expected for geopotential height under geostrophic turbulence theory.

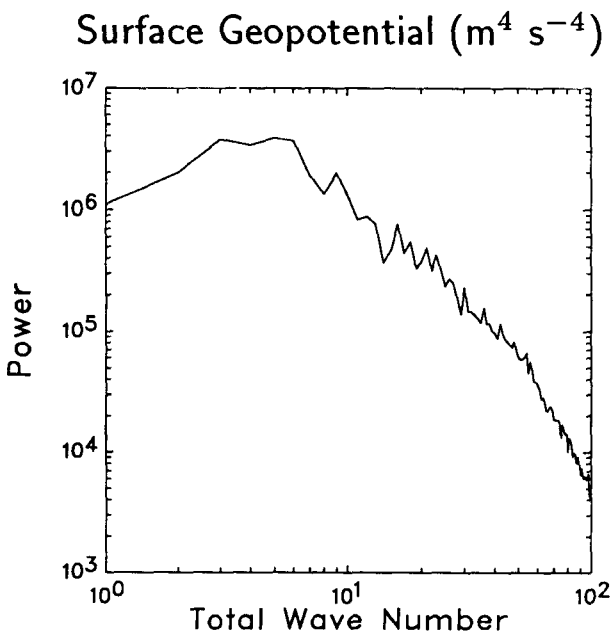

FIG. 1. Spatial spectrum of surface geopotential in m^4 s^{-4} with the total wavenumber n along the abscissa ranging from 1 to 100. Note the logarithmic scales.

In Fig. 2 total spectra are shown for the geopotential height for January and July at 1000, 500, 200, and 10 mb. In the troposphere, the low wavenumber regime exists for waves 1 to 9, while a power law can be fit reasonably well at higher wavenumbers. At 1000 mb the slope is close to -3, at 500 mb it varies from -4 to -5, and at 200 mb the slope is -5. At 10 mb there is no region that clearly shows a power law behavior, although the slope is clearly less than at 200 mb and is ~ -4 or so. Note the great similarity in power in both January and July in the troposphere except for a small increase in July at 1000 mb beyond wavenumber 40. There is more power at nearly all wavenumbers at 10 mb in July. Otherwise, at low wavenumbers in the troposphere, there are noticeable and significant differences between the January and July spectra that relate to the differences in circulation between the two hemispheres with season (see also Boer and Shepherd 1983).

Figure 3 presents the total and mean kinetic energy (KE) spectra for January at 850 and 200 mb, for July at 200 mb, and for the divergent component of KE, KE_D, at 200 mb for January. Both KE and KE_D are shown together with the same vertical scales at 300 mb for January and July in Figs. 4 and 5. As expected, the KE spectra are dominated by the rotational part of the KE, and KE_D is two orders of magnitude smaller at most wavenumbers, although the difference is only about a factor of 5 at wavenumber 100 at 300 mb. For KE_D, up to about wavenumber 6, the stationary component accounts for one- to two-thirds of the variance. Almost all the KE variance comes from the stationary component for waves 1 to 5. However, beyond about wave 10 to wave 80 the stationary component is more than an order of magnitude less than the transient component at 200 mb, and is also much less at 850 mb.

At 850 mb, a power law behavior for the total KE is apparent for wavenumbers higher than 10 with a slope of ~ -2.1. At 200 mb, in both January and July, for wavenumbers 12 to 70 there is a slope close to -3. A much higher slope is evident at very high wavenumbers. Note also the significantly higher power at 200 versus 850 mb at all but the highest wavenumbers. Differences exist between January and July KE spectra

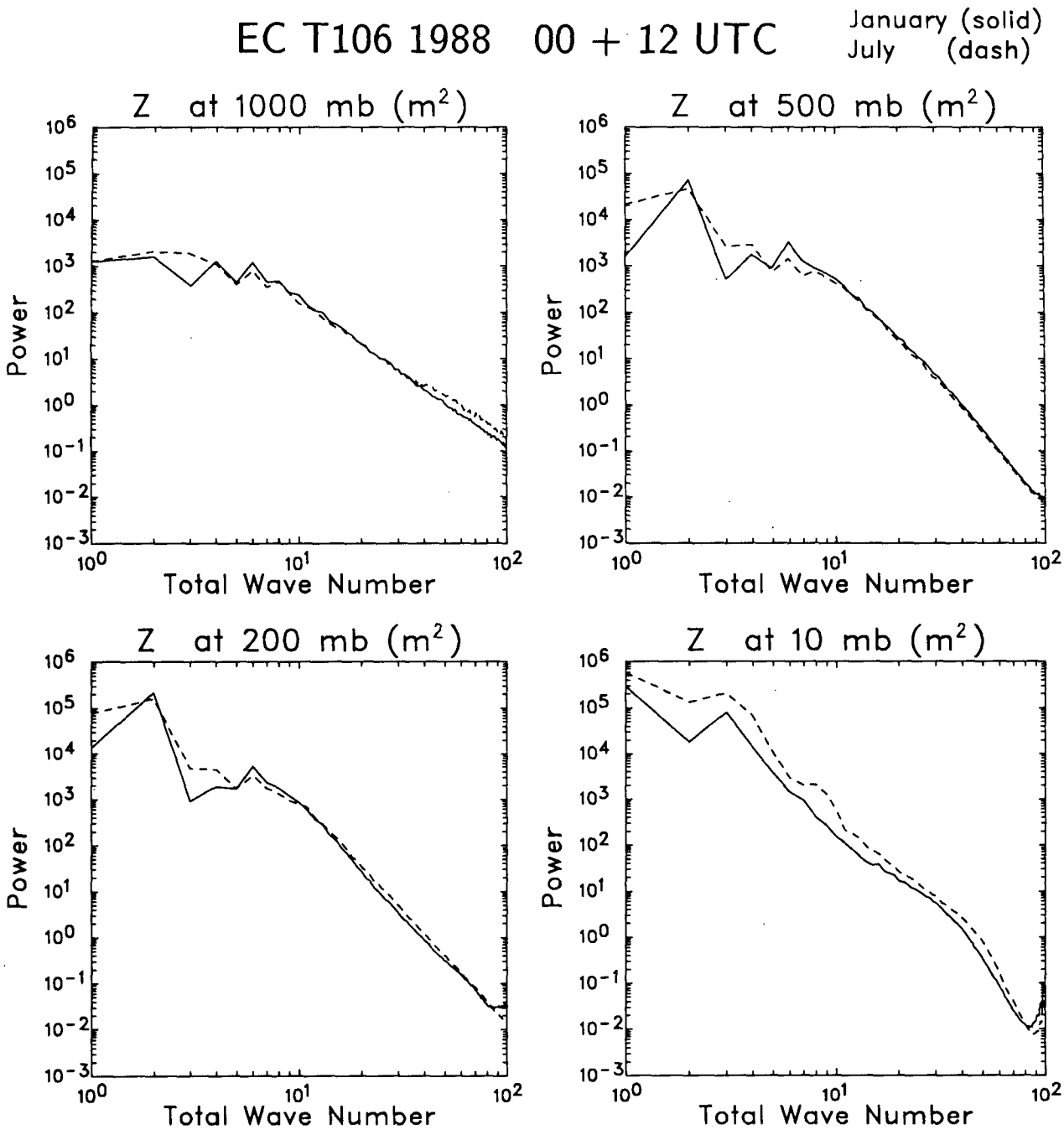

FIG. 2. Time-average spectra for January (solid) and July (dashed) 1988 for geopotential height at 1000, 500, 200, and 10 mb; units: m^2.

at 200 mb, with much more power at $n = 1$ and 5 in January, and more power at $n = 2$ and 3 in July. For KE_D a power law approximation can be found for waves 10 to 70 with a slope of ~ -2.

Also presented in Figs. 4 and 5 are spectra for temperature at 850 and 200 mb, the divergence at 850 and 200 mb, and ω at 500 mb. For ω the total spectrum from the uninitialized analyses is presented as well as the spectra from the initialized analyses out to wave 42.

For temperature, the slope is clearly larger at 200 mb, and averages about -3 for waves 15 to 70 whereas it is closer to -2 at 850 mb. For omega, the uninitialized analyses feature a broad peak between waves 7 and 50,

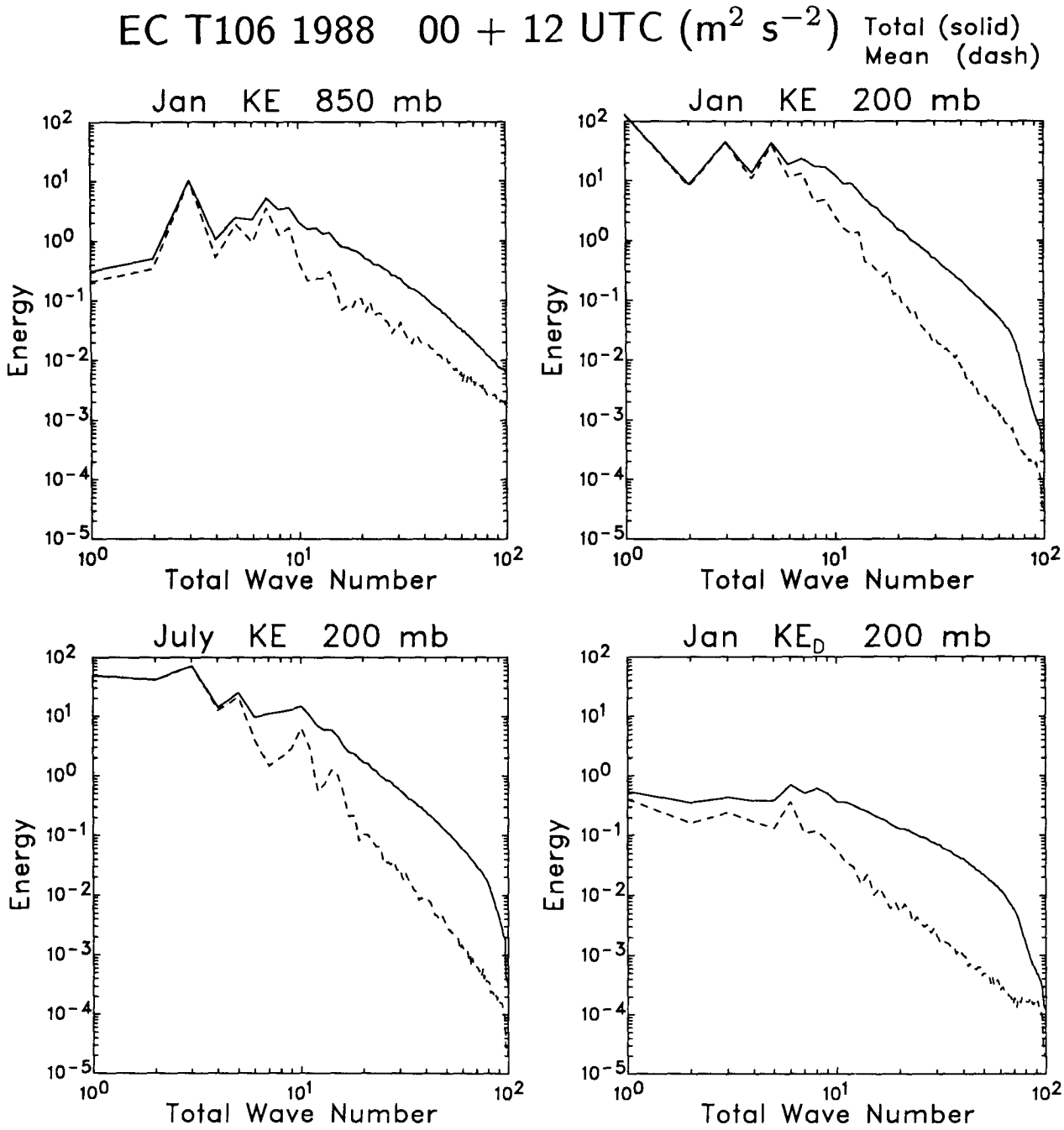

FIG. 3. Time-average spectra for kinetic energy showing the total (solid) and mean (dashed) (i.e., spectrum of the time-average field) spectra for January at 850 mb (top left), January at 200 mb (top right), July at 200 mb (lower left), and January divergent kinetic energy at 200 mb (lower right) in m^2 s^{-2}.

but the power falls off beyond wave 6 for the initialized analyses. Even at low wavenumbers, there is considerably less power in the initialized analyses. The vertical motion is, of course, directly related to the divergence field whose power steadily increases with wavenumber out to about wave 40. At 850 mb, in particular, there is considerable power at all high wavenumbers. The differences between the spectra for ω initialized versus uninitialized serve to emphasize that a lot of the power at the higher wavenumbers for both the divergence and ω is probably noise. That is not to say that there should not be a lot of power at the high wavenumbers, but it

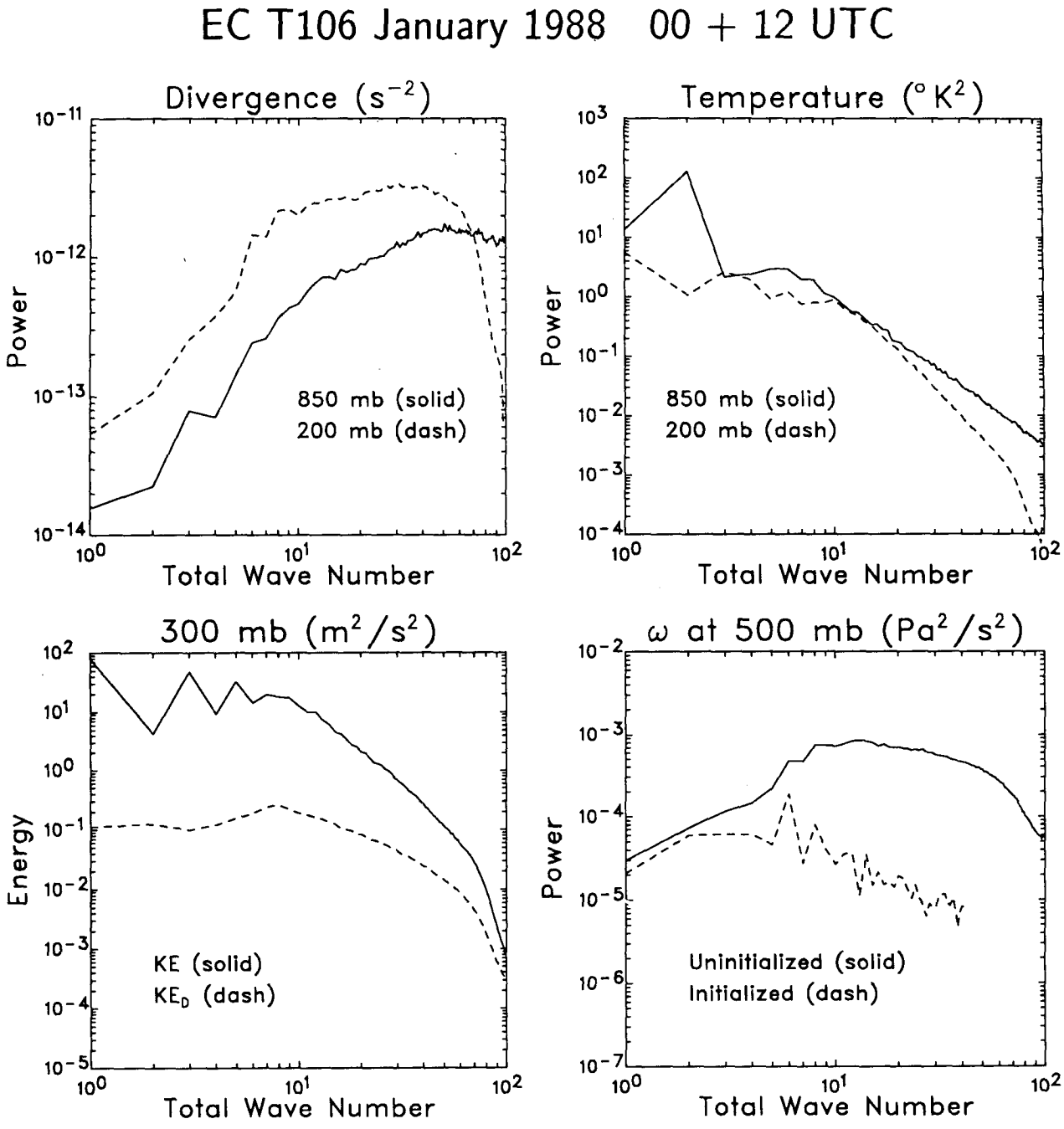

FIG. 4. Time-average spectra for January for divergence (top left) at 850 (solid) and 200 mb (dashed) in s^{-2}, temperature (top right) at 850 (solid) and 200 mb (dashed) in K^2, kinetic energy at 300 mb (lower left) for the total (solid) and divergent (dashed) components in $m^2\ s^{-2}$, and ω at 500 mb for the uninitialized (solid) and initialized (dashed) in $Pa^2\ s^{-2}$.

does indicate that we do not know what form it really takes in the atmosphere. As shown by Trenberth (1991), the equation of continuity linking the divergence with ω is not well satisfied in these analyses, primarily because of the interpolation from sigma to pressure surfaces, so that a lot of the noise arises simply from numerical methods and finite vertical resolution. Nevertheless, a truncation of these fields at T20, for instance, clearly ignores most of the field. Also, as noted earlier, for three-dimensional turbulence the divergence power should increase with increasing wavenumber, and there is some evidence for this in Figs. 4 and 5.

Spectra have also been computed for specific humidity q and relative humidity RH (not shown). Be-

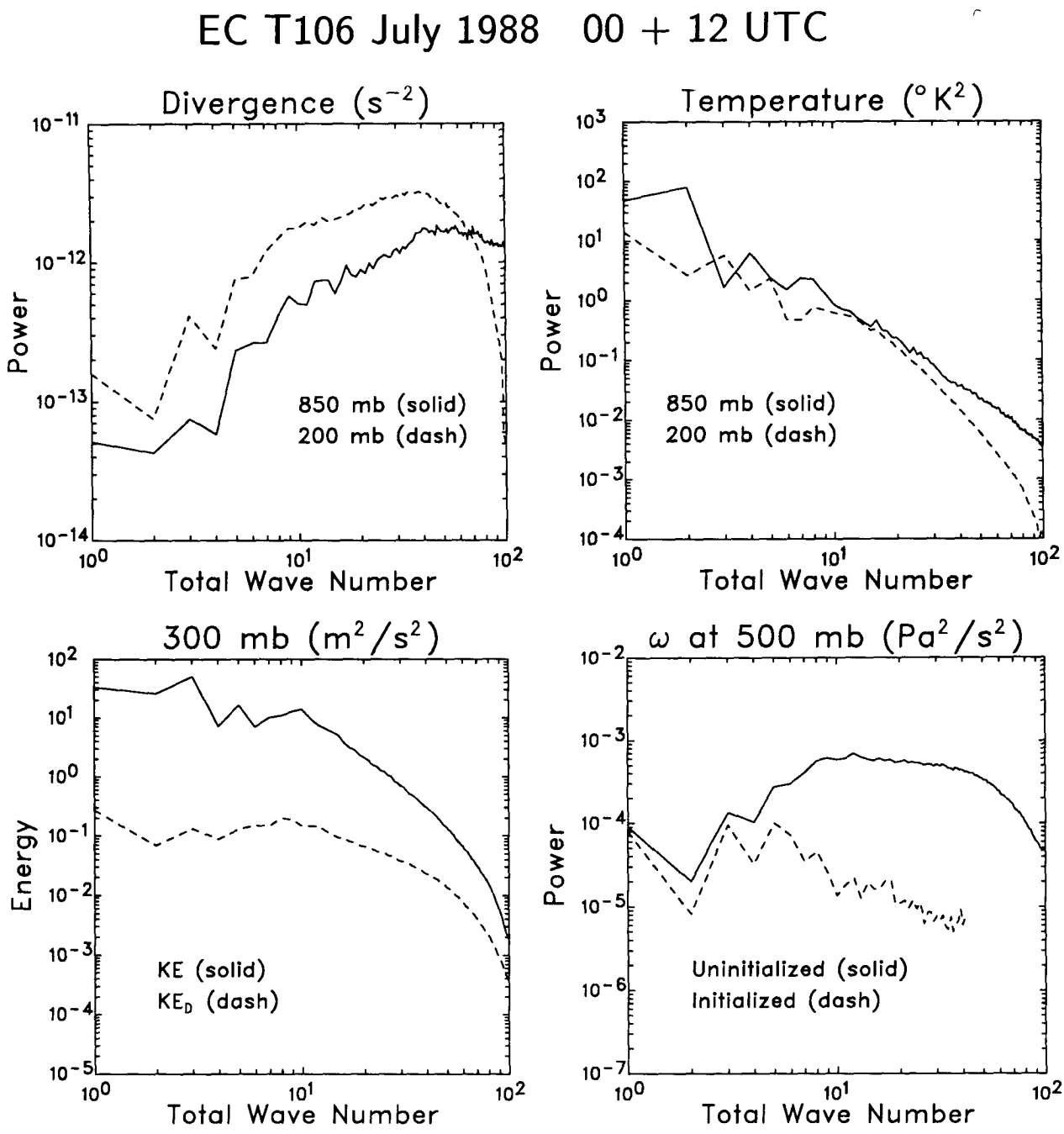

FIG. 5. Time-average spectra for July for divergence (top left) at 850 (solid) and 200 mb (dashed) in s^{-2}, temperature (top right) at 850 (solid) and 200 mb (dashed) in K^2, kinetic energy at 300 mb (lower left) for the total (solid) and divergent (dashed) components in $m^2\ s^{-2}$, and ω at 500 mb for the uninitialized (solid) and initialized (dashed) in $Pa^2\ s^{-2}$.

cause of its dependence on temperature, q peaks at very low wavenumber and falls off by at least two orders of magnitude by wave 40. The RH spectra feature strong power out to wave 10 but fall off by only about one order of magnitude by wavenumber 40. In addition, there is a sharp upturn beyond wave 90 with power at wave 106 only a factor of 20 less than at the peak in the 1000- and 850-mb spectra. This high level of noise has relevance for interpreting Fig. 8, presented later.

To reveal aspects of the stratospheric flow, Fig. 6 shows several spectra for January and July at 10 mb; Fig. 2 shows the z spectra at 10 mb. Unlike the troposphere, at both 50 (not shown) and 10 mb, there is

no clear evidence of a power law behavior in either total or divergent kinetic energy or for temperature. Instead the power starts to fall off sharply beyond about wave 30. Also, in view of the strong asymmetries between the hemispheres in the stratosphere (easterlies in the summer and westerlies in the winter hemisphere), there is no reason to expect the turbulence theory outlined earlier to be relevant. The power in ω peaks quite sharply between total wavenumbers 10 and 15 at both 10 and 50 mb. Most of the ω power is a maximum in zonal wavenumbers 1 and 2, but there is also considerable power in zonal wavenumbers 3 to 7 which contributes to the total wavenumber peak. It is possible that this is associated with forcing of the

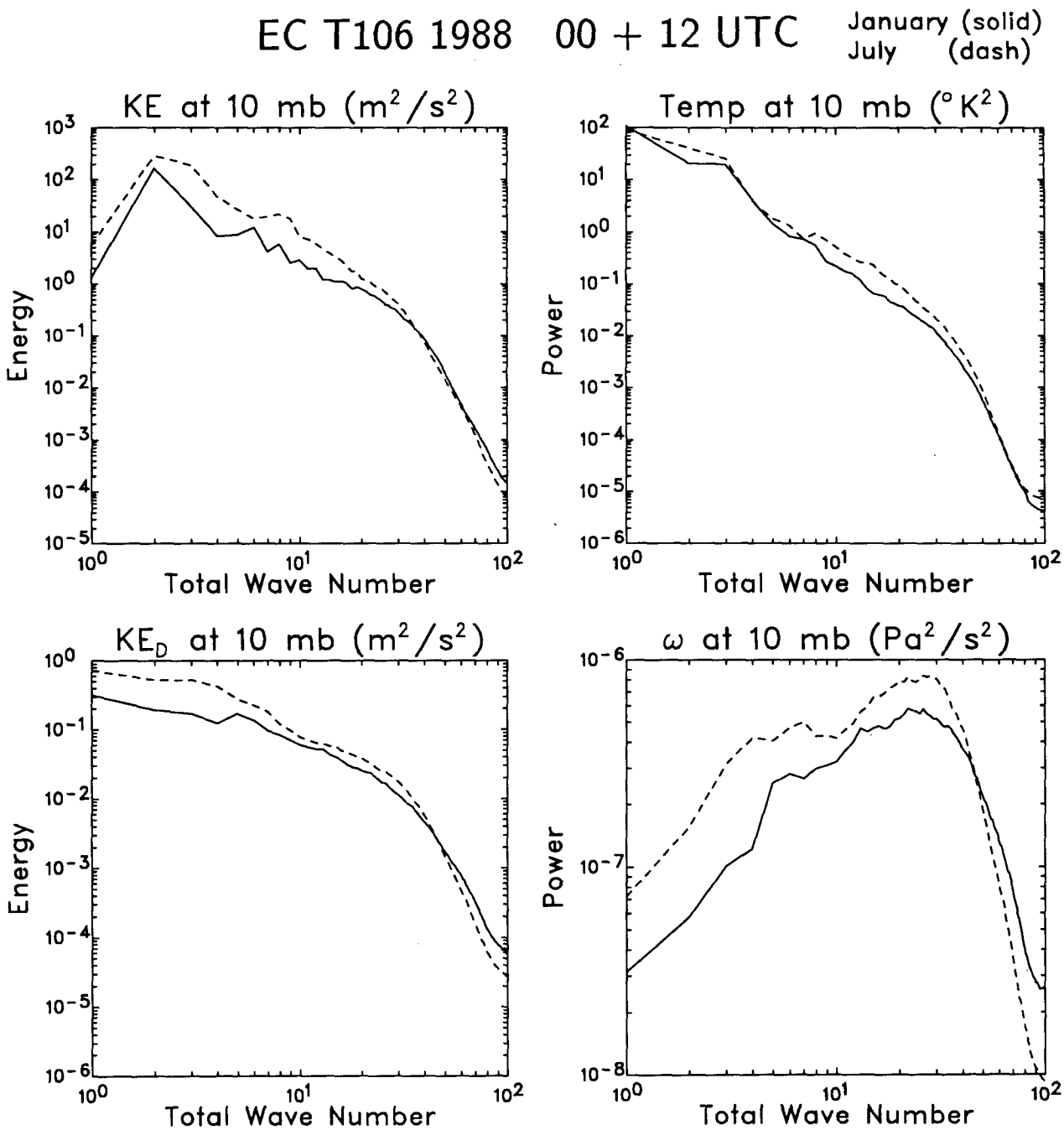

FIG. 6. Time-average spectra for January (solid) and July (dashed) at 10 mb for total kinetic energy (top left) $m^2 s^{-2}$, temperature (top right) K^2, divergent kinetic energy (lower left) $m^2 s^{-2}$, and ω uninitialized (lower right) $Pa^2 s^{-2}$.

stratosphere by transient and quasi-stationary waves originating in the troposphere. However, the 10-mb analyses are no doubt influenced by the fact that it is the top level of the ECMWF model and there are only sparse data available.

To gain some appreciation of the stability of the spectra from one year to the next, Fig. 7 presents the total kinetic energy spectrum at 300 mb for each January of 1986, 1987, 1988, and 1989, all plotted as dashed curves for waves 1 to 42; the mean spectrum for all four years is shown as the solid curve. There is virtually no variability for waves 1–3, and the only noticeable variability is near wavenumber 13. At least in terms of the overall shape of the spectrum, the one-year estimates are quite stable.

Boer and Shepherd (1983) found that the slopes of their kinetic energy spectra were considerably less than estimated in previous studies. The slopes in the KE spectra in our results (Table 1) are not as shallow as in Boer and Shepherd throughout most of the troposphere, although there is an almost monotonic increase in slope with height to the maximum at 200 mb. Although a wider wavenumber range has been used for our results in Table 1, as can be seen from Fig. 3, results are not affected by that. Above 100 mb the slope varies with wavenumber and cannot be well defined. Like Boer and Shepherd, our results feature a maximum slope of ~ -3 near the tropopause, with a shallower slope in the lower stratosphere. Clearly, the changes that have occurred in the global analyses since 1979, analyzed by Boer and Shepherd, have mainly influenced the lower troposphere, and the more recent analyses have more power at higher wavenumbers (i.e., they are less "smooth").

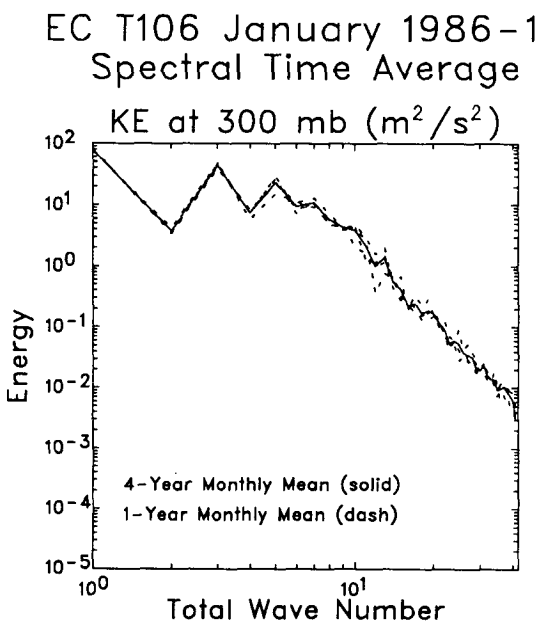

FIG. 7. Time-average spectra for January of kinetic energy showing the total for each of the four years 1986, 1987, 1988, and 1989 (dashed) and their four-year average (solid) in $m^2 s^{-2}$.

TABLE 1. Slope of straight line fit to the kinetic energy spectrum from the current study for waves n = 14 to 40 for January 1988 and from Boer and Shepherd (1983) for waves n = 14 to 25 for January 1979.

Pressure (mb)	This study	Boer and Shepherd
100	−2.2	−2.2
150	−2.7	−2.6
200	−3.0	−3.0
250	−2.9	−2.9
300	−2.9	−2.6
400	−2.6	−2.3
500	−2.6	−2.1
700	−2.5	−1.9
850	−2.1	−1.7
1000	−1.9	−1.5

Based on the spectra, some tentative conclusions can be drawn about the effects of different resolutions on (i) depicting the field, and (ii) making calculations, such as quadratic products with the field. The latter are relevant for flux quantities, for instance. Because the spectra depict variance, a quadratic accuracy to $\sim 1\%$ is achieved roughly where the power drops to less than 1% of the maximum (or strictly speaking, the sum over all the wavenumbers, but this tends to be dominated by the maximum because of the logarithmic scale), whereas the amplitudes in the field itself would be accurate to only $\sim 10\%$. These will be explored further for specific cases below.

For geopotential height (Fig. 2), a T42 truncation excludes waves that contain power three (at 1000 mb) or more than four (at 200 mb) orders of magnitude less than on the large scales and clearly should be adequate. Even a T20 truncation should be sufficient for z for many purposes, although at 1000 mb this would encompass waves ranging over less than two orders of magnitude in power. Because of the slower fall off with n for kinetic energy (Fig. 3) and temperature (Figs. 4 and 5), a truncation at T20 may sometimes be unsatisfactory at some levels by excluding 4% (or more) of spatial variance which corresponds to waves with amplitudes of 20% of the maximum. At T42 truncation, however, even at 850 mb for kinetic energy (Fig. 3), the missing waves would be two or more orders of magnitude smaller in power. For the divergent motion field, including vertical velocity (Figs. 4 and 5), a low-order truncation such as T20 would be unacceptable by excluding most of the power, and even a T42 truncation can be questioned, although we believe that the higher wavenumber power is mostly unphysical noise.

3. Spectral truncation of ECMWF data

The data in the ECMWF WCRP archive are available in spectral coefficient form at T106 resolution.

For a scalar field it is then straightforward to truncate to any particular wavenumber resolution, simply by changing J in (1).

For a vector field, such as velocity, spectral truncation is more involved, especially as the truncation for velocity should be effected in terms of vorticity ζ and divergence δ, not velocity.

In spectral representation, most numerical weather prediction models use vorticity and divergence as predictors in place of the velocity components. However, ECMWF has chosen to archive the spectral coefficients for

$$U = u\cos\phi \tag{7a}$$

$$V = v\cos\phi. \tag{7b}$$

Note that the $\cos\phi$ factor is necessary so that these components are zero at the poles and they can therefore be represented in spherical harmonics. The use of the velocity representation complicates the process of truncating the fields to a different resolution, and it can lead to very large errors in u, v near the poles, where $\cos\phi \to 0$.

The U and V are represented as

$$U = a \sum_{m=-J}^{+J} \sum_{n=|m|}^{J+1} U_n^m Y_n^m \tag{8a}$$

$$V = a \sum_{m=-J}^{+J} \sum_{n=|m|}^{J+1} V_n^m Y_n^m, \tag{8b}$$

and using recursion relationships (e.g., Washington and Parkinson 1986), it can be shown that

$$U_n^m = +(n-1)\epsilon_n^m \psi_{n-1}^m - (n+2)\epsilon_{n+1}^m \psi_{n+1}^m + im\chi_n^m, \tag{9a}$$

$$V_n^m = -(n-1)\epsilon_n^m \chi_{n-1}^m + (n+2)\epsilon_{n+1}^m \chi_{n+1}^m + im\psi_n^m, \tag{9b}$$

where

$$\epsilon_n^m = \left(\frac{n^2 - m^2}{4n^2 - 1}\right)^{1/2}. \tag{9c}$$

Because U and V are obtained by differentiating streamfunction and velocity potential, it is necessary to include an extra north–south mode (for n) in (8) compared with (1), as can be seen in (9).

It is straightforward, using (9) or equivalent, to compute the velocity spectral coefficients from the vorticity or divergence coefficients. However, it is not straightforward to invert (9) and solve for expressions for ψ_n^m and χ_n^m in terms of U_n^m and V_n^m. In the ECMWF analyses, U_n^m and V_n^m are given. In order to carry out a self-consistent truncation to some other wavenumber J, say by reducing J from 106 to 42, it is necessary to truncate the velocity components U_n^m and V_n^m at $J = 41$ waves. The first 41 coefficients are sufficient to determine a 42nd coefficient for both vorticity and divergence, which, in turn, through (9), determines the appropriate 42nd and 43rd coefficients of U_n^m and V_n^m. In practice we have done this by spectrally transforming the 41 coefficients to a Gaussian grid then transforming back to spectral space and, in the process, computing the requisite coefficients. Given all the U and V coefficients, we can reconstruct the fields on a grid and compute u and v. It is worth reiterating that any departure from these procedures can lead to inconsistencies in the coefficients which can be manifest as huge errors near the poles. The difference between a velocity field that has been properly truncated and one with the unadjusted truncated coefficients projected directly onto the T42 grid are as large as 25 m s^{-1} near the poles.

Of particular concern is the improper use of the ECMWF software distributed with the WCRP dataset that allows the projection of fields directly onto a regularly spaced grid (which can be readily modified to be a Gaussian grid). This procedure uses the full T106 resolution data to provide the gridpoint values and does not do a truncation. In particular, if output is desired on a 2.5° grid, for example, then a truncation to T47 (or lower) waves is essential first in order to avoid unrepresentative gridpoint values. Alternatively, the data should be placed onto a T106 grid (320 by 160 points) and appropriately smoothed *before* interpolation to the new grid.

As noted in the introduction, the global ECMWF analyses are being made available on a 2.5° grid, but the value assigned to each grid point is the exact value at T106 resolution. This is a case where application of the appropriate truncation is not at the user's command. As an example, Fig. 8 presents the 1000-mb relative humidity analyses on 16 November 1989, first, as made available on the 2.5° grid, and second, as truncated from T106 at T42 and then projected onto the same grid. The former field is identical to one projected at T106 resolution directly onto the 2.5° grid, whereas the latter is suggested as more appropriately truncated for a grid of this size. The differences in structure are large and readily apparent in many places.

It is noteworthy also that the analyses contain relative humidity values more than 5% outside of physical limits (i.e., negative values and values over 100%) which apparently arise from the spectral character of the field. The user is advised to test the relative humidity field and ensure that values are changed to be within the physical limits.

4. Discussion and conclusions

Given knowledge of the spectrum, informed decisions can be made about the appropriateness of smoothing for presenting fields. One method of

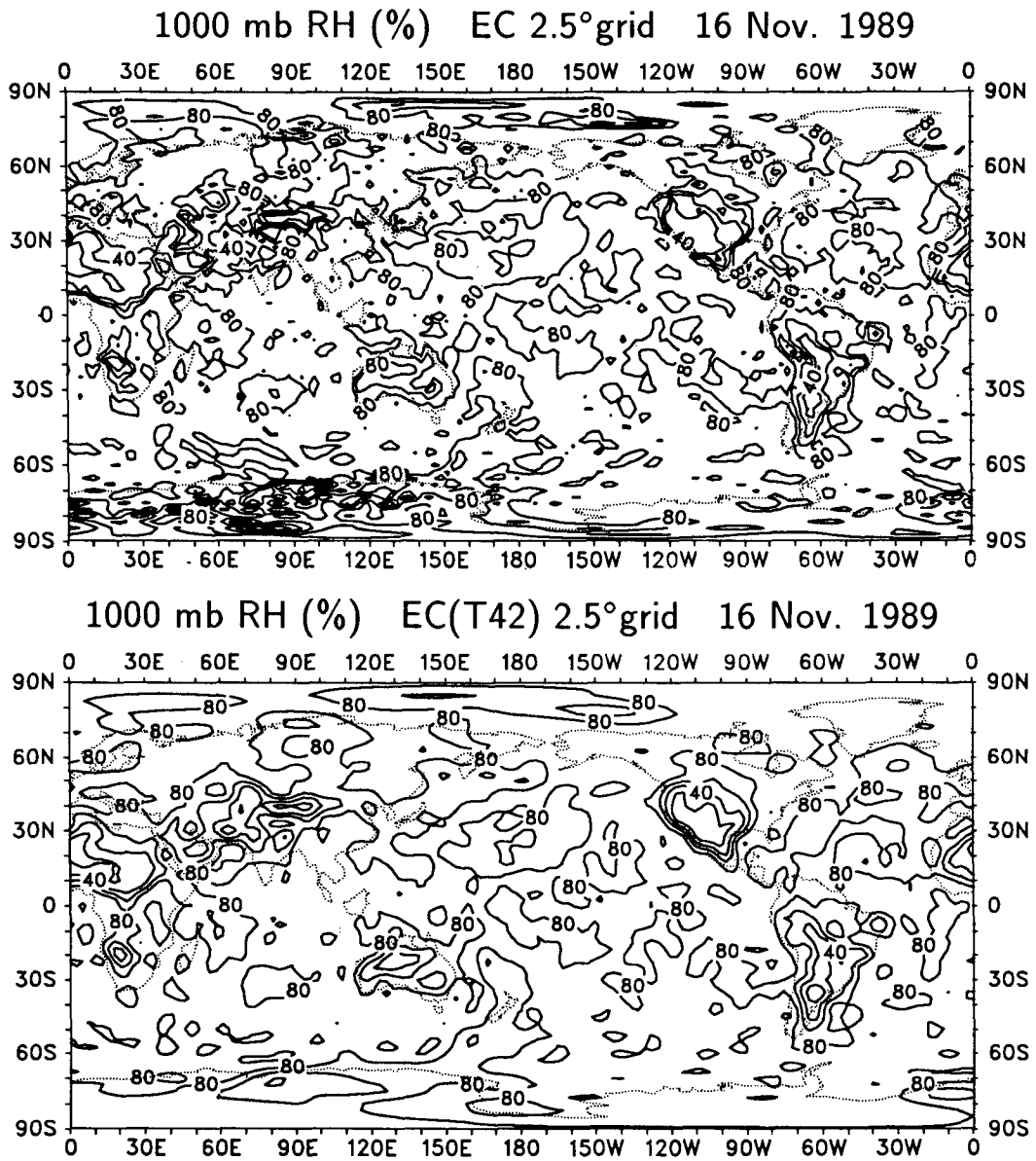

FIG. 8. The relative humidity fields at 1000 mb on 16 November 1989 in percent as depicted on the 2.5° grid and as truncated at T42 resolution. The contour interval is 20%.

smoothing in spectral space is where the fields are truncated at some other resolution, preferably with a tapered weighting function near the truncation limit in order to avoid "ringing" effects if there is spectral power on those scales (Sardeshmukh and Hoskins 1984). For many purposes, truncations at T21 are found to be suitable for revealing features of interest. Occasionally, the larger scales may still be masked by smaller scales considered to be noise, and we have then utilized a truncation at T12. On the other hand, if details are important, such as those near topography, truncations at T31 are often sufficient to bring out those features.

A field from Trenberth (1991) is used to illustrate the results through the use of spectral truncation (Fig. 9). It represents the mass divergence required to make the mass budget balance in May 1988 using twice-daily data. At low (T12) resolution (Fig. 9) it reveals the strong spectral peak at wave 2 associated with the semidiurnal tide that is not removed when averaging only twice-daily data. However, at wavenumbers 7 and above, the spectral power is within an order of magnitude of the spectral peak, so the pattern is gradually lost as more wavenumbers are added. Some evidence of the signal is present at T21, but even there the noise

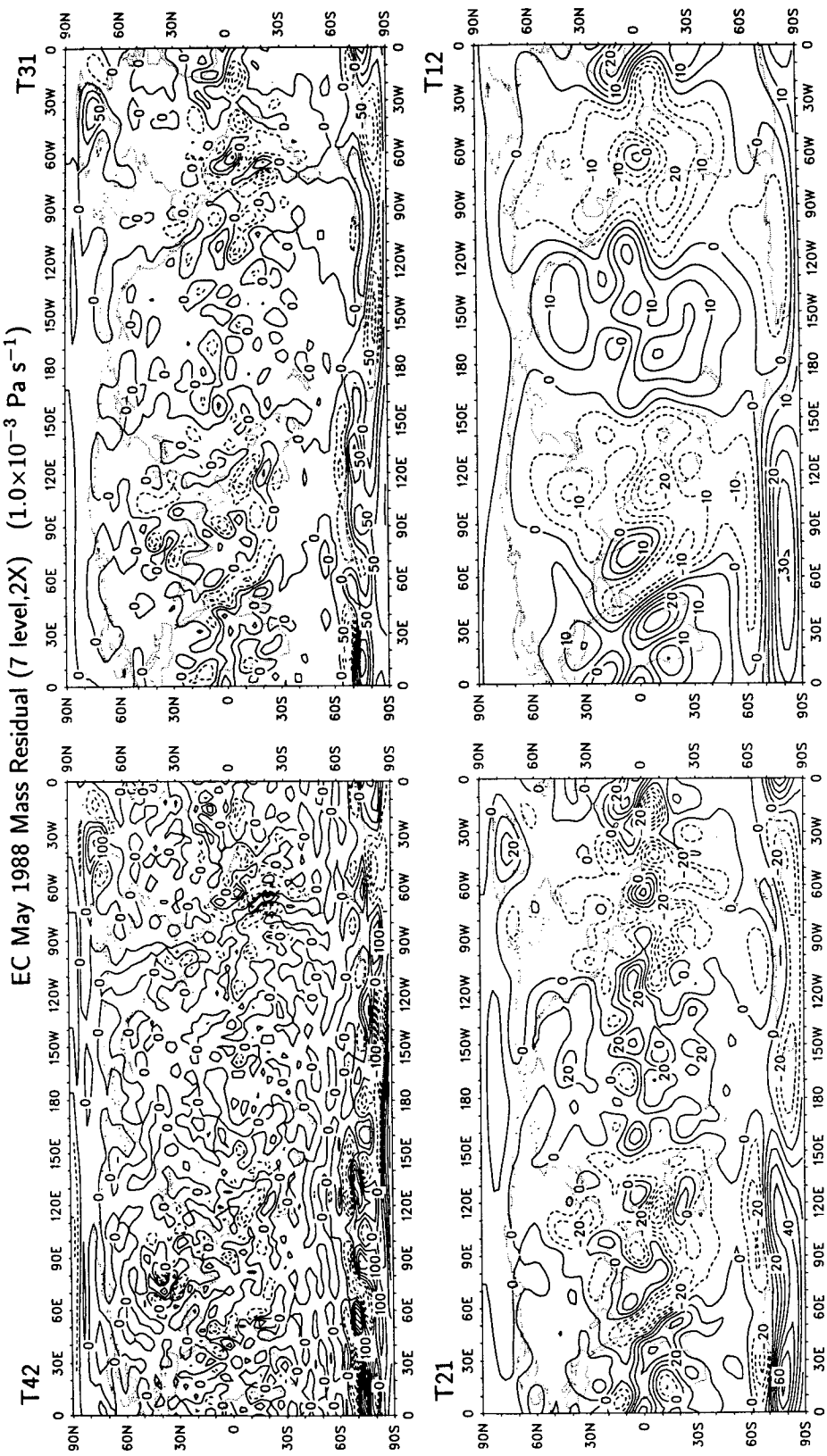

FIG. 9. The residual to the vertically integrated mass budget for May 1988 from twice-daily data, in 10^{-3} Pa s^{-1} at four resolutions, T42, T31, T21, and T12. The contour intervals are 50, 25, 10, and 5 ($\times 10^{-3}$ Pa s^{-1}), respectively. Negative contours are dashed.

is considerable. At T42 resolution it is impossible to pick out the pattern at all.

We have presented spatial spectra as depicted by the ECMWF global analyses. Almost certainly these spectra depart somewhat from the real atmospheric spectra because of the nature of the four-dimensional data assimilation system and the processes (like diffusion) included in the model, but also because of noise introduced in the archival process of interpolating to pressure surfaces. Nevertheless, it is likely that most of the spectra represent a good approximation to the real world and it is clearly seen that the spectra can be classified in broad ways.

In most atmospheric spectra, it is possible to identify a low wavenumber regime that does not follow a power law and which is dominated by the stationary forced part of the flow. A higher wavenumber regime where an approximate power law does appear to hold can also often be identified. For the rotational part of the flow in the upper troposphere, the observed spectra follow quite closely that expected for quasi-two-dimensional quasigeostrophic turbulence between about wavenumbers 12 and 70, with a kinetic energy spectrum falling off as n^{-3}, and it seems appropriate to interpret this as the inertial subrange (Boer and Shepherd 1983) although with the qualifications noted by Shepherd (1987). At higher wavenumbers, information comes from the model and is determined by the model physics and the parameterization of subgrid-scale processes. Some evidence of aliasing and/or "spectral blocking" was found in some fields, while for other fields the drop-off in power is more than expected. This may indicate insufficient dissipation in some fields and too much in others in the NWP model involved in the ECMWF data assimilation. There is no evidence of the transition from a -3 slope in the kinetic energy and temperature spectra to $-5/3$ for scales smaller than several hundred km, as found by Gage and Nastrom (1986); however, those scales are near the resolution limit (wave 100) here.

In the lower troposphere, there is more power at high wavenumbers than would be expected from quasi-two-dimensional turbulence and this is interpreted as due to the influence and close proximity of the lower boundary so that not only inertial effects are present, but also direct forcings and effects due to such things as the formation of sharp gradients in frontal systems at the boundary. In the stratosphere also, perhaps not unexpectedly, the spectra at high wavenumbers do not follow a power law behavior very well.

One focus here has been the implications of these spectra for the processing and display of data and results. There are also implications for the archival and retrieval of fields, and it has been shown that the 2.5° gridded fields made available by ECMWF do not properly take the structure in the fields into account, leading to aliasing and excessively noisy fields in several cases. Procedures have been described for truncating scalar and vector fields, given the available archive, and we recommend that spectral transform techniques should be used for processing the data wherever possible. Consequently, the fields should be converted to the appropriate Gaussian grid. For spectral coefficients, we have described how to truncate consistently to any particular resolution.

It is found that T42 resolution is adequate resolution for most quantities of interest in climate diagnostics. But clearly there is structure lost at T42 for the ω, divergence, and moisture fields, although it is uncertain whether this structure is meaningful or simply mostly represents noise. In contrast, T21 or R15 resolution is often not adequate although can be very useful for displaying results where the interest is only in the larger scales.

Acknowledgments. This research is partially sponsored by the NOAA Tropical Oceans Global Atmosphere Project Office under Grant NA87AANRG0208. The data were supplied by ECMWF.

REFERENCES

Boer, G. J., and T. G. Shepherd, 1983: Large-scale two-dimensional turbulence in the atmosphere. *J. Atmos. Sci.*, **40**, 164–184.

Boville, B. A., 1991: Sensitivity of simulated climate to model resolution. *J. Climate*, **4**, 469–485.

Charney, J. G., 1971: Geostrophic turbulence. *J. Atmos. Sci.*, **28**, 1087–1095.

Gage, K. S., and G. D. Nastrom, 1986: Theoretical interpretation of atmospheric wavenumber spectra of wind and temperature observed by commercial aircraft during GASP. *J. Atmos. Sci.*, **43**, 729–740.

Gray, B. M., and R. A. Madden, 1986: Aliasing in time-averaged tropical pressure data. *Mon. Wea. Rev.*, **114**, 1618–1622.

Kolmogorov, A. N., 1941: The local structure of turbulence in incompressible viscous fluid for very large Reynolds numbers. *C. R. Acad. Sci. URSS*, **30**, 301–305. [*Dokl. Akad. Nauk. SSSR*, **30**(4), 299–303].

Sardeshmukh, P. D., and B. J. Hoskins, 1984: Spectral smoothing on the sphere. *Mon. Wea. Rev.*, **112**, 2524–2529.

Shepherd, T. G., 1987: A spectral view of nonlinear fluxes and stationary–transient interaction in the atmosphere. *J. Atmos. Sci.*, **44**, 1166–1178.

Tennekes, H., 1978: Turbulent flow in two and three dimensions. *Bull. Amer. Meteor. Soc.*, **59**, 22–28.

Trenberth, K. E., 1973: Global model of the general circulation of the atmosphere below 75 kilometers with an annual heating cycle. *Mon. Wea. Rev.*, **101**, 287–305.

——, 1991: Climate diagnostics from global analyses: Conservation of mass in ECMWF analyses. *J. Climate*, **4**, 707–722.

——, 1992: Global analyses from ECMWF and atlas of 1000- to 10-mb circulation statistics. NCAR Tech. Note NCAR/TN-373+STR, 191 pp plus 24 fiche.

——, and J. G. Olson, 1988a: An evaluation and intercomparison of global analyses from NMC and ECMWF. *Bull. Amer. Meteor. Soc.*, **69**, 1047–1057.

——, and J. G. Olson, 1988b: ECMWF global analyses 1979–1986: Circulation statistics and data evaluation. NCAR Tech. Note NCAR/TN-300+STR, 94 pp plus 12 fiche.

Washington, W. M., and C. L. Parkinson, 1986: An Introduction to Three-Dimensional Climate Modeling. University Science Books, 422 pp.